

A Virtual Physics-based Approach to Multiple Odor Sources Localization

Xiaoping Ma¹, Yuli Zhang^{*1,2}, Yanzi Miao¹

¹School of Information and Electrical Engineering, China University of Mining and Technology, Xuzhou, China

²School of Science, Dalian JiaoTong University, Dalian, China

*Corresponding author, e-mail: zhangyuli1021@hotmail.com

Abstract

The detection of an odor source location has been enhanced by using multiple plume-tracing mobile robots. So far, many researchers focus on locating a single source in varied environments. The present study is concerned with the problem of multiple chemical sources localization using multi-robot system. In this study, multiple groups of robots were used and coordinated by a multi-robot cooperation strategy with virtual physics force, which includes structure formation force, goal force, repulsion force and rotary force. In order to test the effectiveness of the proposed strategy, plume model with two sources was constructed by computation fluid dynamics simulations. Simulation experiment discussed the influence of the varied frequencies of wind direction/ speed and methane release with different initial positions of multiple groups to the search performance. Simulation comparison experiments using three kinds of plume tracing algorithms: chemotaxis, anemotaxis and fluxotaxis were carried out respectively and the comparative result about three plume tracing algorithms was illustrated.

Keywords: virtual physics force, plume tracing, source localization, mobile robot

Copyright © 2014 Institute of Advanced Engineering and Science. All rights reserved.

1. Introduction

The recent increasing threat of hazardous chemical agents that are released into an environment has highlighted the need for superior detection of hazardous emission sources. Odor source localization using plume-tracing robots has the potential to detect such dangerous odor released from sources such as explosives, toxic or harmful gas and fire. Hayes et al. [1] broke down odor source localization into three subtasks: plume finding-coming into contact with the odor, plume traversal-following the odor plume to its source and source declaration-determining from odor acquisition characteristics that the source is in the immediate vicinity. Many obstacles have hindered odor source localization in the past two decades. Such as the unstable wind in the natural environment, the detection of the odor and the wind with mobile robots. In this paper, the experiments were setup on the assumption of a strong and constant velocity but varying directional airflow in the environment. Meanwhile, the robots can detect the odor and the wind precisely.

So far, many plume-tracing research has focused on locating a single source and many strategies and methods have been designed, such as gradient-following-based strategy (chemotaxis) [2, 3], combination of chemotaxis and anemotaxis [4, 5], infotaxis [6], evolutionary approach [7], model-based strategy [8, 9], multiple robots cooperation based on swarm intelligence [10, 11], virtual physics based strategy [12-14], and strategy fusing vision information [15]. While many of these algorithms would likely succeed in finding one source even in a multi-source environment, they offer no guidance on how to partition the robots during a search to ensure that all sources are located in minimal time, how to avoid obstacles and other robots during global search, and how to continue searching for other sources once a source has been found, and how to avoid re-finding the same source. In this problem, the intensity of each source may vary with time and the position of the source may be occluded by obstacles or other robots. The above-mentioned multi-source problem involves a variety of distinct challenges that have received little attention in the single source literature.

This paper discusses an extension of our earlier work on multiple odor sources localization using virtual physics based robots, published recently in *Advanced Materials Research* [16], which had discussed a new approach based virtual physics for coordinating two groups of mobile robots in the searching of two methane sources in open environment. The results told us that the swarm behavior used in the proposed approach ensured the robots detect all sources. Here, we focus on the detailed analysis of the collaborative control and give more simulation comparison experiments on three algorithms: chemotaxis, anemotaxis and fluxotaxis at three different frequencies of wind direction/ speed and methane release with six different initial positions of multiple groups, and the results show that the proposed strategy can effectively navigate the mobile robotics swarms to the chemical sources and the comparative result about three plume tracing algorithms is illustrated.

2. Research Method

2.1. The Simulation Arenas

The plume model adopted in this study to test the control strategies was developed by [17]. This plume was simulated using a computation fluid dynamic (CFD) software package, FLUENT (Fluent, Inc.). The plume data produced by Fluent CFD were imported into MATLAB (Mathworks, Inc.) and integrated with simulated mobile robots model for pluming tracing behavior simulation. The gas in this paper was methane (CH_4). The simulation environment we used in the paper (figure 5) was a 2D environment of $20\text{m} \times 20\text{m}$. The positions of methane sources were (1, 11) and (3, 9). Two sources had the same release rates which were $500 \text{ kg} / \text{m}^3\text{-s}$. Varying airflow directions were adopted instead of the fixed airflow direction; the varying airflow entered into the left-hand side boundary of the domain at a constant 5m/s velocity but varied directions between $\pm 22.5^\circ$ during the simulation and existed from the right-hand side boundary of the domain. From figure 5 we can see that, the plumes from the two sources are converged together, which make the group robots can not tell which source the plume they detected comes from. So, one odor source can be tracked by more than one group. This is pointless the waste of time with two groups for only a single source. Hence, the delay in searching the next odor can possibly occur. The new proposed strategy with forbidden area setting should cope with this disadvantage.

2.2. The Control Algorithms

The strategy based virtual physics we have proposed consists of the following three parts: plume finding, plume traversal and odor source declaration.

2.2.1. Plume Finding

At the beginning, when the robot finds no plume, the robot would perform passive monitoring [18] to find plume, that is, the robot remains stationary and waits for an odour plume to intersect the robot's current location. The male silkworm moth employs this strategy. When trying to detect the plume of pheromone released by the female silkworm moth, the male moth waits, head into the wind in an exposed position, until it detects the pheromone.

2.2.2. Plume Traversal

To make searching time faster, we are using parallel search by two groups' robots. Each group has six robots and a virtual robot, and then there is total twelve robots used for two odor source localization. Each group runs by itself. Members of each group send and take information among their group. If one group found and locate a source, the group would stop moving.

2.2.2.1. The Control Algorithms Based Virtual Physics for each Group of Robots

The control algorithms based virtual physics for each group of six robots developed by [14] for robots are adopted in this study. The control force includes two kinds of effort, which are virtual structure force $F(VS)$ (acting on the six robots) and virtual goal force $F(VG)$ (acting on the virtual robot).

Virtual structure force $F(VS)$ can be stated as follows:

$$\begin{cases} F'_{xk}(VS) = \sum_{i=1, i \neq k}^6 k_r \frac{q_k q_i}{d_{ki}^2} \cos(\theta_{ki}) - k_s (x_k - x_c) ((x_k - x_c)^2 + (y_k - y_c)^2 - r^2) \\ F'_{yk}(VS) = \sum_{i=1, i \neq k}^6 k_r \frac{q_k q_i}{d_{ki}^2} \sin(\theta_{ki}) - k_s (y_k - y_c) ((x_k - x_c)^2 + (y_k - y_c)^2 - r^2) \end{cases} \quad (1)$$

Where k_r , k_s are positive gain, q_k and q_i are the K -th and i -th electric charges ($q_k = q_i = 1$ in this paper), and d_{ki} is the distance between them, (x_k, y_k) is the position of robot k .

$$\cos(\theta_{ki}) = \frac{x_k - x_i}{|d_{ki}|}, \sin(\theta_{ki}) = \frac{y_k - y_i}{|d_{ki}|}.$$

The force defined in (1) makes the robot move toward the circle with center (x_c, y_c) and radius r when $(x_k, y_k) \neq (x_c, y_c)$ and form a regular hexagon.

We obtained united vector as follows:

$$(F'_{xk}(VS), F'_{yk}(VS)) = \frac{(F'_{xk}(VS), F'_{yk}(VS))}{\|(F'_{xk}(VS), F'_{yk}(VS))\|} \quad (2)$$

Virtual goal forces $F(VG)$ are constructed by different plume-tracing algorithms: chemotaxis, anemotaxis and fluxotaxis respectively. The specific construction method of $F(VG)$ is defined as follows:

Chemotaxis: The gradient strategy simply follows the chemical gradient, so the direction of the largest chemical concentration is the goal direction. The virtual robot receives the sensor data available on robot k ($k=1, 2, 3, \dots, 6$), chooses the robot j who has the highest concentration and moves toward it a distance of step length s_7 . The virtual goal force is defined as follows:

$$F(VG) = \frac{X_j(t) - X_v(t)}{\|X_j(t) - X_v(t)\|} \quad (3)$$

Where X_v and X_j are positions of virtual robot and robot j . $\|\cdot\|$ represents the Euclidean norm operator.

Anemotaxis: The intuition behind the anemotaxis is to move the lattice upstream while keeping the robots inside the plume. If the gas concentrations all robots sensed exceeded a predefined threshold ρ_T and the wind velocities were not all zero, The virtual robot receives the sensor data available on robot k ($k=1, 2, 3, \dots, 6$), records all the wind velocities: $\vec{v}_1, \vec{v}_2, \dots, \vec{v}_6$ and calculates the average wind velocity $\bar{\vec{v}} = \frac{1}{6} \sum_{i=1}^6 \vec{v}_i$. Then the virtual robot chooses upwind direction

$-\bar{\vec{v}}$ and moves toward it a distance of step length s_7 . The virtual goal force is defined as follows:

$$F(VG) = -\frac{\bar{\vec{v}}}{\|\bar{\vec{v}}\|} \quad (4)$$

fluxotaxis: In this paper, six robots composed of regular hexagon grids. The formula of calculating mass flux by a robot is:

$$\rho \bar{\vec{v}} \cdot \vec{n} = \rho |\bar{\vec{v}}| \cos \theta \quad (5)$$

Where ρ and $\bar{\vec{v}}$ are chemical concentration and wind velocity of the robot respectively. \vec{n} and θ are shown in Figure 1.

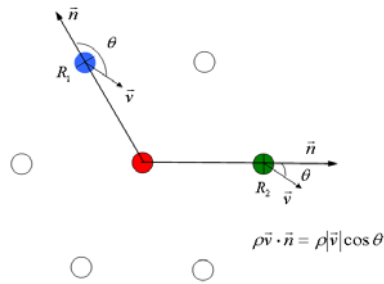


Figure 1. The Method of Calculating Flux by a Robot

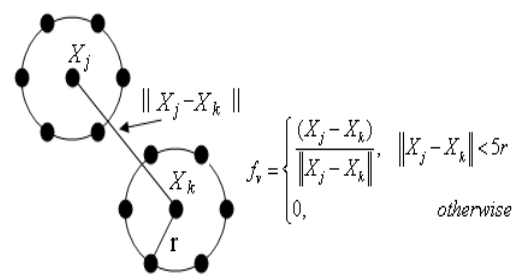


Figure 2. The Method of Calculating Repulsion Force between the Virtual Robots of Two Groups

If the gas concentrations all robots sensed exceeded a predefined threshold ρ_T and the wind velocity was not zero, the virtual robot following the robot i with minimal negative mass flux will take the robots upwind which towards the source. Then the virtual robot chooses the robot i with minimal negative mass flux and moves toward it a distance of step length s_1 . The virtual goal force is defined as follows:

$$F(VG) = \frac{X_i(t) - X_v(t)}{\|X_i(t) - X_v(t)\|} \quad (6)$$

Then, the discrete-time model of the virtual robot movements can be stated as:

$$X_v(t+1) = X_v(t) + s_1 \cdot F(VG) \quad (7)$$

Where $X_v(t+1)$ and $X_v(t)$ are positions of the virtual robot at time step $t+1$ and t .

As the virtual robot moved to a new position, the robots would also move a distance of step length s_2 under the action of the virtual structure force $F(VS)$.

So, the discrete-time model of the robot movements can be stated as:

$$X_k(t+1) = X_k(t) + s_2 \cdot F_k(VS) \quad (8)$$

Where $X_k(t+1)$ and $X_k(t)$ are position of the robot k ($k=1, 2, 3, \dots, 6$) at time step $t+1$ and t .

It should be noted that step length s_1 of the virtual robot should less than that of the robots s_2 such that the robots can follow it.

2.2.2.2. The Control Algorithms Based Virtual Physics between each Group of Robots

Parallel Search with repulsion force: Parallel search logically makes searching time faster. Several groups of robot run and find odor sources separately. But, robot groups run separately can make one group cannot find the other and will not know if it goes to the same odor source as the others. It is very inefficient that one odor source can be tracked by more than one group. In addition, the robots from one group are movable obstacles because robots have a physical shape and foot print of finite size, the other group must avoid collisions with them. In order to guarantee of the positions of one group's robots to be away from the other, we assume that there is a repulsion force f_v between the virtual robots. The repulsion force f_v between the virtual robots of two groups is defined as follows:

$$f_v = \begin{cases} \frac{(X_j - X_k)}{\|X_j - X_k\|}, & \|X_j - X_k\| < 5r \\ 0, & \text{otherwise} \end{cases} \quad (9)$$

Where X_k and X_j are positions of virtual robots of two groups. $\|\cdot\|$ represents the Euclidean norm operator. The specific calculation process is shown in Figure 2.

Then, the virtual goal force is modified by:

$$F'(VG) = F(VG) + f_v \quad (10)$$

Parallel Search with repulsion force and forbidden area setting: Although repulsion force between the virtual robots of two groups can guarantee the positions of one group's robots to be away from the other, it can not guarantee one odor source to be tracked by only one group. Considering the case shown in figure 3, we assume that, the group first located a source is denoted by group1 and the source which was first located is denoted by source 1. So, when the distance between two virtual robots is less than $5r$, by analyzing the forces $F'(VG)$ of the virtual robot of group 2, we can explain this problem.

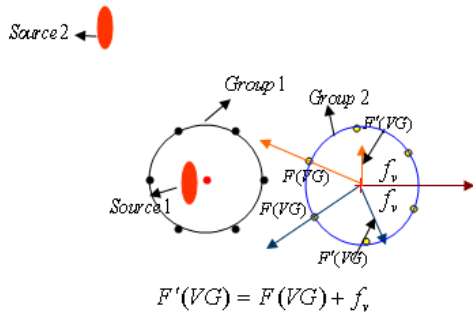


Figure 3. The Method of Calculating Forces of the Virtual Robot of Group 2

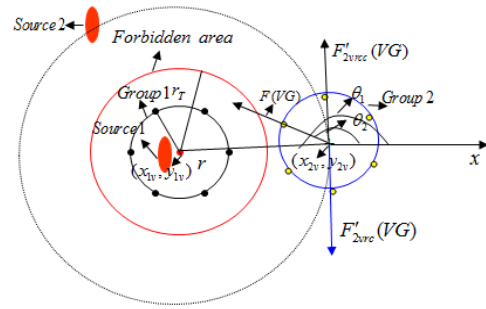


Figure 4. The Method of Setting the Forbidden Area and the goal force $F'_{2vr}(VG)$ of Group 2' Virtual Robot

The circular forbidden area is its center at the virtual robot of group 1 and radius r_T ($r_T > r$) which is shown as follows:

$$(x - x_{1v})^2 + (y - y_{1v})^2 \leq r_T^2 \quad (11)$$

Where (x_{1v}, y_{1v}) is the position of the virtual robot of group1.

In order to bypass the source1, we modified the goal force $F'(VG)$ of group 2' virtual robot as the rotary force f_{2vr} , which is shown as follows:

$$f_{2vr} = f_{x2vr}i + f_{y2vr}j \quad (12)$$

The following equations express the direction of the rotary force in two different conditions:

$$\begin{cases} f_{x2vr} = f_{x2vrc}, f_{y2vr} = f_{y2vrc} & \theta_1 \leq \theta_2 \\ f_{x2vr} = f_{x2vrcc}, f_{y2vr} = f_{y2vrcc} & \theta_1 > \theta_2 \end{cases} \quad (13)$$

Where (f_{x2vrc}, y_{2vrc}) is clockwise force and (f_{x2vrcc}, y_{2vrcc}) is counter clockwise force. θ_1 is the angle between the positive direction of x-axis and the line connected two virtual robots of two groups in counterclockwise direction. And θ_2 is the angle between the positive direction of x-axis and the goal force $F'(VG)$ of the group 2 in counterclockwise direction.

$$\begin{cases} f_{x2vrc} = (y_{2v} - y_{1v}) \\ f_{y2vrc} = -(x_{2v} - x_{1v}) \end{cases} \quad (14)$$

And,

$$\begin{cases} f_{x2vrcc} = -(y_{2v} - y_{1v}) \\ f_{y2vrcc} = (x_{2v} - x_{1v}) \end{cases} \quad (15)$$

Where (x_{1v}, y_{1v}) and (x_{2v}, y_{2v}) are the positions of the virtual robot of group1 and group 2 respectively.

Let us normalize it as follows:

$$F'_{2vr}(VG) = \frac{f_{x2vr}}{|f_{2vr}|} i + \frac{f_{y2vr}}{|f_{2vr}|} j \quad (16)$$

We can see, when $|\theta_1 - \theta_2| < \pi/2$, group 2 by force $F'_{2vr}(VG)$ can successfully bypass source 1 and locate source 2. It should be noted that once the virtual robot of group 2 chose a rotary method (clockwise or counter clockwise), it should keep on until it escaped from source 1. When $|\theta_1 - \theta_2| > \pi/2$, group 2 by force $F'(VG)$ can successfully move away from source 1.

2.2.3. Source Declaration

Plume source identification is the process whereby the robots identify the odor source in the environment. This paper adopted source identification in [12], which tell us that, if the robots surround a suspected emitter, and the total mass flux measured by the sensor grid consistently exceeds some small, empirically-determined threshold Φ_T in a given number of steps n_s , then the robots have localized the emitter.

3. Results and Analysis

In this section, we will test the search efficiency of the proposed multi-robot system based virtual physics force at three different frequencies of wind direction/ speed and methane release, which are: standard frequency, twice frequency and treble frequency. In addition, different initial positions of two groups will also have great influence on the search efficiency. So, we give six kinds of initial positions (position of the virtual robot), which are: Position1 (18,4), (18,14), denoted by P1; Position2 (18,10), (18,14), denoted by P2; Position3 (18,4), (18,10), denoted by P3; Position4 (18,14), (18,16), denoted by P4; Position5 (18,8), (18,10), denoted by P5; Position6 (18,4), (18,6), denoted by P6; Two groups with P1 have maximum spacing, then P2 and P3, then P4-P6.

By simulating extensive numerical search trials for each parameter, we chose the parameter given by able 1.

Table 1. Parameters of Algorithm

k_c	r	k_r	s_1	s_2	ρ_T	Φ_T	n_s
0.0001	0.3[m]	5	0.06[m]	0.12[m]	0.005[kg/m ³]	0.05[kg/m ² ·s]	10

3.1 Chemotaxis

To get a better understanding of the effect that we proposed parallel search has on the plume tracing task, we give a series of snap shots of the tracing odor plumes process of the two groups' robot using chemotaxis in simulation environment. As a sample, we introduce the tracing odor plumes process at the treble frequency with six initial positions respectively shown in Figure 5. Twelve robots are indicated by "o" and two virtual robots are indicated by "+".

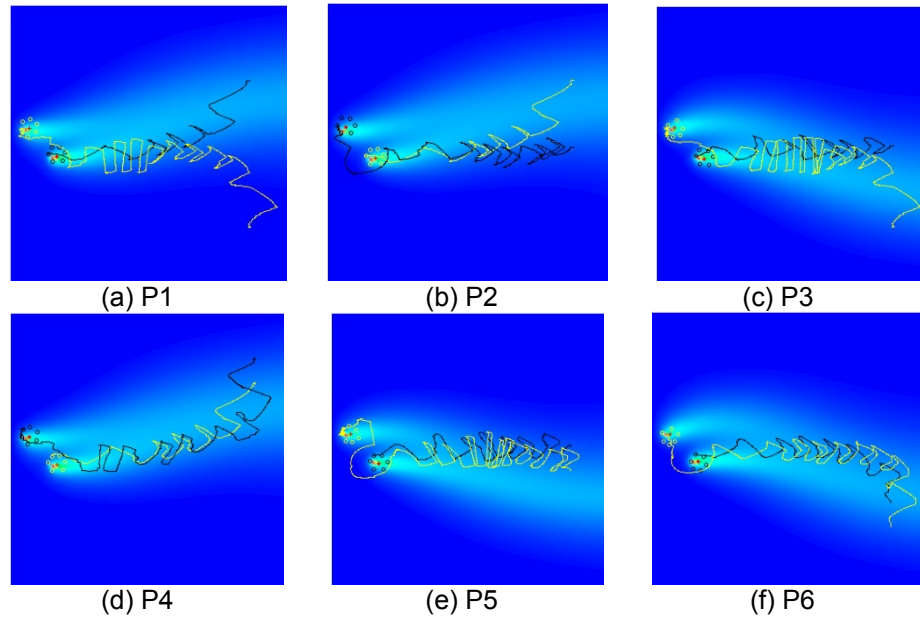


Figure 5. Plume Tracing Paths using Chemotaxis at the Treble Frequency with Six Initial Positions

Then, we give the search time used by sources locating at three different frequencies with six different initial positions respectively.

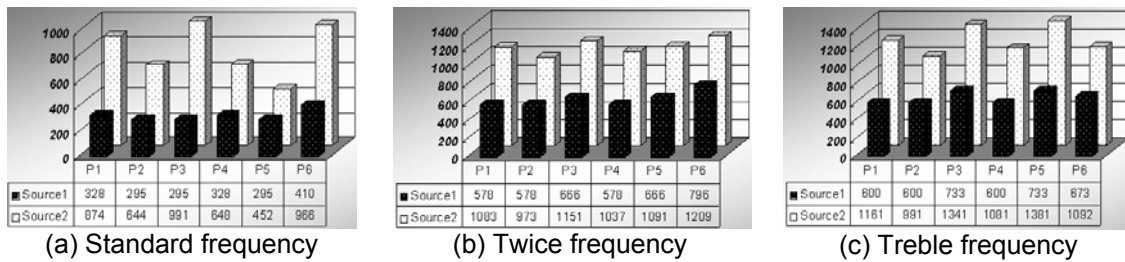


Figure 6. Comparisons on Search Time used by Locating Two Sources using Chemotaxis at Three Different Frequencies with Six Different Initial Positions

Figure 5-6 tell us that, the proposed search strategy using chemotaxis is effective and obtains 100% success rate; in addition, with the increasing of the wind direction/ speed frequency and methane release frequency, the search time used by the robots increases. The main reason is that the increasing of the wind direction/ speed frequency and methane release frequency make the plume drift up and down drastically, the robots using the chemotaxis move towards the direction of the largest chemical concentration which make the tracing paths similar to the variation pattern of the wind direction. For example, the average time is 780s under the case the wind direction/ speed frequency and methane release frequency is standard frequency, while the average search time is 1180s under the case the wind direction/ speed frequency and methane release frequency is treble frequency. Considering six different initial positions we had tested, Groups start out from P3 spent the most time to locate two sources and groups start from P2 spent the least time even at three different frequencies of wind direction/ speed and methane release. For example, the average time is 1040s with P1, 870s with P2, 1160s with P3, 920s with P4, 970s with P5, and 1090s with P6 under the case the wind direction/ speed frequency and methane release frequency is treble frequency. The main reason is that P1, P3 and P6 have a same coordinate (18,4) which is farthest from two sources; the farther the initial positions from two sources the longer time should be spent to located them.

In addition, take account of search efficiency with P1, P3 and P6, two groups with P1 have maximum spacing. Closer positions always make two groups come in contact with each other and the repulsion force between the virtual robots of two groups repels each other which leads to the groups spent more time to find all the sources. So, different initial positions of two groups using chemotaxis also exert great influence on the search efficiency.

3.2. Anemotaxis

Figure 7 gives the plume tracing paths of two groups of robots using anemotaxis at the treble frequency with six initial positions respectively.

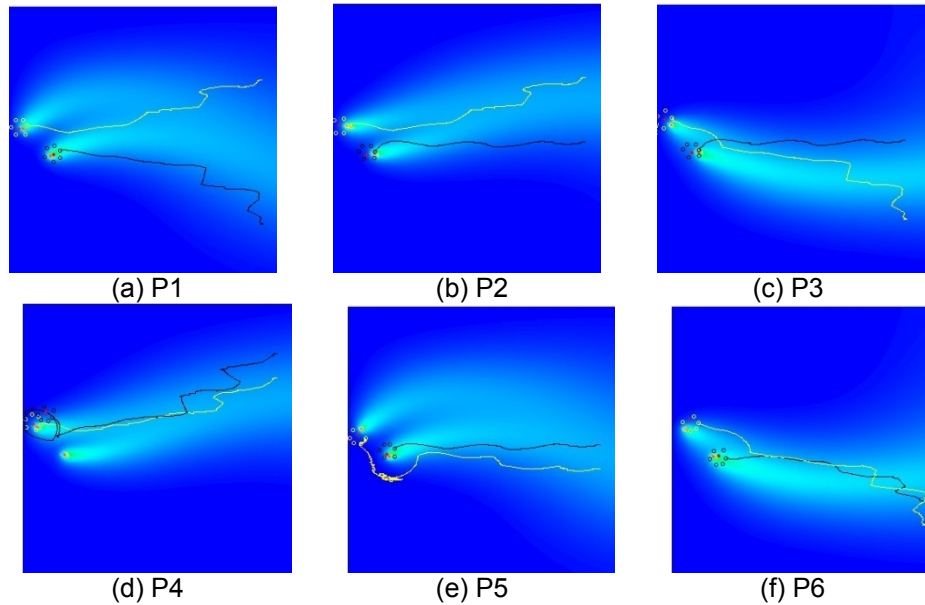


Figure 7. Plume Tracing Paths at the Treble Frequency with Six Initial Positions

Figure 8 gives the search time used by sources locating at three different frequencies with six different initial positions respectively.

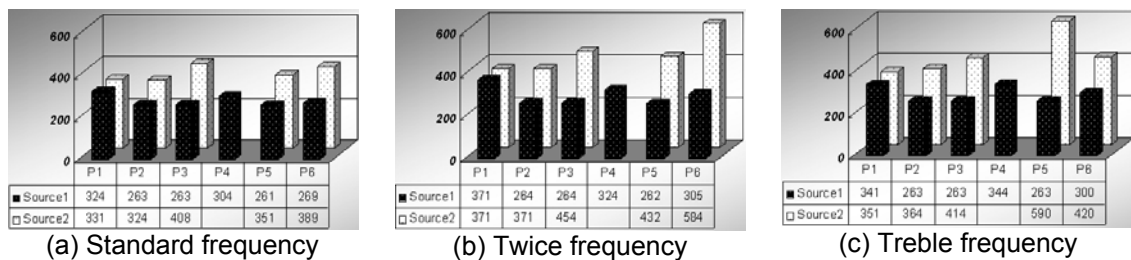


Figure 8. Comparisons on Search Time used by Locating Two Sources using Anemotaxis at Three Different Frequencies with Six Different Initial Positions

Figure 7-8 tell us that anemotaxis obtains 100% failure rate at three different frequencies with initial position P4, while anemotaxis is effective and obtains 100% success rate with other five different initial positions. The main reason is that, P4 is at upper right corner of the area which is close to the above source and two groups with initial position P4 are quite close. So, the plume-tracing path of two groups are almost the same. Anemotaxis which moving towards the upwind direction makes two groups all located the same source that is located

upwind the other source. Forbidden area and rotary force could not guarantee the group to find the source downwind to the located source (anemotaxis makes the robots to move towards the upwind direction, not downwind direction) and the search failed. Considering initial positions except for P4, with the increasing of the wind direction/ speed frequency and methane release frequency, the tracing paths of the robots using anemotaxis is very similar to each other, so the search time used by the robots is also similar. The main reason is that the increasing of the wind direction/ speed frequency and methane release frequency make the plume to high concentrations which always exceeded threshold ρ_T and the robots using the anemotaxis move towards the upwind direction which make the two groups run and find odor sources separately and make the search time increase slightly. The average time are less than 400s at three different frequencies of wind direction/ speed frequency and methane release which is far less than the groups using chemotaxis. Groups start out from P1 spent the least time to locate two sources, then groups start from P2 and P3, then groups start from P5 and P6. For example, the average time is 350s with P1, 390s with P2 and P3 and 460s with P5 and P6. So, more dispersed initial positions of two groups can make the anemotaxis more effective in parallel search than the chemotaxis.

3.3. Fluxotaxis

Figure 9-10 give the plume tracing paths and search time of two groups of robots using fluxotaxis at the standard frequency, twice frequency and treble frequency with three different initial positions respectively.

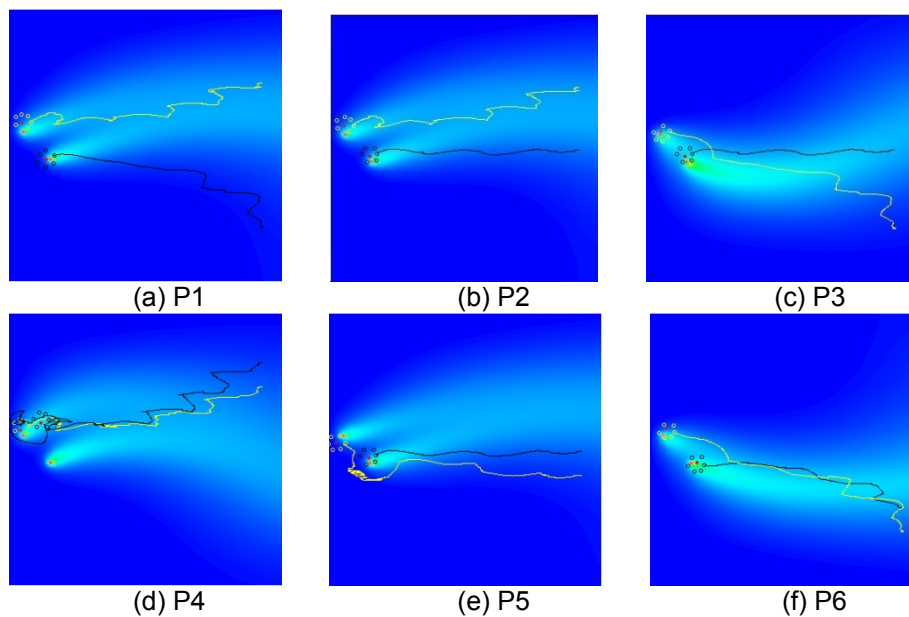
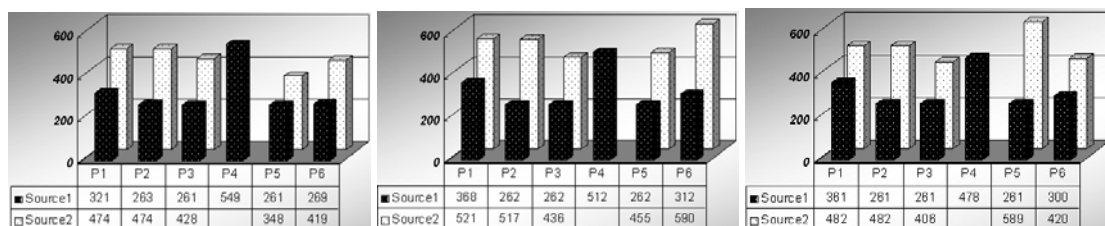


Figure 9 Plume Tracing Paths using Fluxotaxis at the Treble Frequencies with Six Different Initial Positions



(a) Standard frequency (b) Twice frequency (c) Treble frequency
 Figure 10. Comparisons on Search Time used by Locating Two Sources using Fluxotaxis at Three Different Frequencies with Six Different Initial Positions

From Figure 9 -10 we can see that, the performance of plume tracing using fluxotaxis is very similar to that of anemotaxis.

Figure 5 -10 tell us that, the proposed multi-robot cooperation strategy with chemotaxis is very effective and obtains 100% success rate at all three different frequencies wind direction/ speed and methane release with six different initial positions. But, the search time using the chemotaxis is much more than that of the anemotaxis and fluxotaxis and also the performance is influenced greatly by different frequencies wind direction/ speed and methane release and the initial positions. The main reason is that the robots using the chemotaxis move towards the direction of the largest chemical concentration which make the tracing path similar to the variation pattern of the wind direction and always first locate the source downwind the other source. Forbidden area and rotary force can guarantee the other group to find the source upwind to the located source. In addition, we can see that the varied wind direction/ speed frequency and methane release frequency exert little influence on the search performance for the robots using fluxotaxis and anemotaxis. A reasonable explanation is that, both fluxotaxis and anemotaxis combine information about wind velocity which can make the two groups run and find odor sources separately and parallelly. Furthermore, more dispersed initial positions of two groups can make the anemotaxis and fluxotaxis more effective in parallel search.

4. Conclusion

Aims of this study are to tackle the challenges of tracing plumes and locate multiple odor sources. In this study a cooperative search strategy based on mobile robotics swarms with virtual physics forces was adopted to control a number of mobile robots to locate two odor sources. A new method for avoiding the one odor source is traced by more than one group is introduced. This method based on a rotary force avoids the robots to re-locate the same source which has been located by other robots, and leads them to move toward other source. Simulation experiments compared three plume-tracing algorithms: chemotaxis, anemotaxis and fluxotaxis and discussed the influence of the varied wind direction/ speed frequencies and methane release frequencies and different initial positions of two groups to the search performance. After conducting the experiments, we may derive the following conclusion from this research: first, the varied wind direction/ speed frequency and methane release frequency exert great influence on the search efficiency for chemotaxis but not for anemotaxis and fluxotaxis; second, more dispersed initial positions of two groups, the more effective by parallel search when using plume-tracing algorithms: anemotaxis and fluxotaxis. In the future, we will choose more groups of robots to multiple odor sources localization in the more complex environment in which intensity of each source may vary with time, the position of the source may be occluded by obstacles or other robots, odor plume may be more turbulent and further, transplant the control strategy on the true swam robots in the experiment arena.

Acknowledgements

This work was financially supported by the National Natural Science Foundation of China under Grant 61303183, the Specialized Research Fund for the Doctoral Program of Higher Education of China under Grant 20120095120023 and Postdoctoral Research Funds of Jiangsu Province under Grant 1101107C.

References

- [1] Hayes AT, Martinoli A, Goodman RM. Distributed odor source localization. *IEEE Sensors Journal*. 2002; 2(3): 260-271.
- [2] Sandini G, Lucarini G, Varoli M. *Gradient Driven Self-Organizing Systems*. Proceedings of the IEEE/RSJ International Conference on Intelligent Robots and Systems. Yokohama. 1993: 429-432.
- [3] Nurmaini S, Tutuko B, Thoharsin A R. Intelligent Mobile Olfaction of Swarm Robots. *IAES International Journal of Robotics and Automation (IJRA)*. 2013; 2(4): 189-198.
- [4] Kuwana Y, Shimoyana I. Pheromone-guided mobile robot that behaves like a silkworm moth with living antennae as pheromone sensors. *International Journal of Robotics Research*. 1998; 17(9): 924-933.
- [5] Hayes AT, Martinoli A, Goodman RM. Swarm robotic odor localization: off-line optimization and validation with real robots. *Robotica*. 2003; 21(4): 427-441.

- [6] Vergassola M, Villermaux E, Shraiman BI. 'Infotaxis' as a strategy for searching without gradients. *Nature*. 2007; 445(25): 406-409.
- [7] De Croon GCHE, O'Connor LM, Nicol C, et al. Evolutionary robotics approach to odor source localization. *Neurocomputing*. 2013; 121: 481-497.
- [8] Marques L, Nunes U, de Almeida A. Olfaction-based mobile robot navigation. *Thin Solid Films*. 2002; 418(1): 51-58.
- [9] Farrell JA, Pang S, Li W. Plume mapping via hidden markov methods. *IEEE Transactions on Systems, Man, and Cybernetics-Part B: Cybernetics*. 2003; 33(6): 850-863.
- [10] Zhang YL, Ma XP, Miao YZ. *Localization of Multiple Odor Sources using Modified Glowworm Swarm Optimization with Collective Robots*. Proceedings of the 2011 Chinese Control Conference. Yantai. 2011: 1899-1904.
- [11] Jovan F, Dhiemas RYS, Alvissalim M Sakti, et al. *Real Multiple Mobile Robots Implementation of PSO Algorithm for Odor Source Localization*. Proceedings of the International Conference on Advance Computer Science and Information Systems. Bali, Indonesia. 2010: 253-257.
- [12] Zarzhitsky D, Spears D, Spears W. *Distributed robotics approach to chemical plume tracing*. Proceedings of IEEE/RSJ international conference on intelligent robots and systems. Alberta. 2005: 4034-4039.
- [13] Zou YH, Chen WH, Luo DH. *A highly flexible virtual physics-based control framework for multi-robot chemical plume tracing*. Proceedings of IEEE international conference on Control and Automation. Christchurch. 2009: 775-779.
- [14] Zhang YL, Ma XP, Miao YZ. Chemical Source Localization using Mobile Robots in Indoor Arena. *TELKOMNIKA Indonesian Journal of Electrical Engineering*. 2013; 11(7): 3718-3727.
- [15] Jiang P, Meng QH, Zeng M, et al. Indoor gas source identification by fusing visual and olfactory information of a mobile robot. *Chinese High Technology Letters*. 2011; 21(8): 867-873.
- [16] Zhang YL, Ma XP. *Localizing Multiple Odor Sources using Virtual Physics based Robots*. Advanced Materials Research. 2013; (756-759): 223-227.
- [17] Liu ZZ, Lu TF. *A simulation framework for plume-tracing research*. Proceedings of the 2008 Australian Conference on Robotics & Automation. Canberra. 2008: 1-7.
- [18] Russell RA, Bab Hadiashar A, Shepherd RL, et al. A comparison of reactive robot chemotaxis algorithms. *Robotics and Autonomous Systems*. 2003; 45(2): 83-97.